INCREASE OF INDUSTRIAL ROBOT ACCURACY BASED ON KINEMATIC ERRORS COMPENSATION

STEPAN CHLADEK[1], JIRI SVEDA[1], ZBYNEK SIKA[2], PETR BENES[2]

[1]Czech Technical University in Prague, Faculty of Mechanical Engineering, Department of production machines and equipment (RCMT), Prague, Czech Republic

[2]Czech Technical University in Prague, Faculty of Mechanical Engineering, Department of Mechanics, Biomechanics and Mechatronics, Prague, Czech Republic

Industrial robots are used in many technical applications from simple pick-and-place tasks to complex machining, welding and assembly applications. The repeatability of the robots is usually high. However, the accuracy is much lower, and it decreases with the robot size selected. Robot calibration represents a possible way to increase accuracy, and two main approaches have been distinguished. Kinematic calibration deals with geometric errors only, and the robot is considered as a rigid body. By contrast, non-kinematic calibration takes into account further sources of errors. This paper deals with kinematic calibration, where an artifact is attached to a robot flange and its position is measured using a laser tracker. The novelty of the method is based on the consecutive rotation of only a single joint, where the artifact trajectory is circular. Real robot geometry is calculated based on identified circles. Numerical simulations seem promising, as well as verification with Stäubli TX2-90, where the accuracy was increased by more than 43%.

KEYWORDS

industrial robot, positioning accuracy and repeatability, robot kinematic calibration, laser tracker measurement, artifact measurement

1 INTRODUCTION

Industrial robots are used in many technical applications. There are an estimated 2.7 million industrial robots in use in 2022, with approximately 400,000 new robots entering the world market every year [Zippia 2022]. They are integrating into different applications, from simply picking and placing objects and to complex assembling, welding, and machining tasks with the highest accuracy requirements.

Industrial robots are considered to run in automatic mode and in processing the selected program. The program may be prepared using online programming through manual motion and teaching of the robot. However, this process is both time consuming and results in robot downtime during the teaching time. Since the target positions are set manually, there is only a requirement for repeatability. Currently, the usual approach is based on the offline programming of robots, where the program is prepared in advance using simulation software. This approach requires high accuracy in robot positioning. Generally, there are more parameters that decrease the resulting accuracy: nominal and real dimensions not exactly matching, the load of the robot, gravity, backlash, encoder errors, and others. High-accuracy application utilization is limited for industrial robots; however, accuracy is hard to find in data sheets. Smaller robot arms tend to be more precise, because small angular errors are multiplied by shorter lengths of the arm. The standard method of industrial robot accuracy enhancement represents a calibration process, which consists of the following [Roth 1987]:

1. Modeling
2. Measurement
3. Error identification
4. Compensation

Modeling can be divided into kinematic and non-kinematic (complete) forms, where the kinematic form solves only geometric parameters (length of robot links, joint offsets) and the robot is considered as a rigid body. By contrast, the non-kinematic form also incorporates compliance parameters. A comparison of the mentioned calibration models was published [Joubair 2013], where the non-kinematic model integrated all geometric parameters and five compliance parameters related to stiffness of the efficiency of the 2nd, 3rd, 4th, 5th and 6th joints and the model was analyzed. The kinematic model for calibration utilized that provided by earlier work [Joubair 2015, Kong 2022, Driels 1993], while the non-kinematic model utilized another work [Nubiola 2013]. These involved 25 geometric error parameters and four compliance parameters of the 2nd, 3rd, 4th, and 5th joints being considered.

Measurements can be made either with or without the use of external devices, where the robot itself provides the measurement. A number of measuring devices exist where laser trackers are typically attached to the robot [Joubair 2013, Nubiola 2013]. The drawbacks of the laser tracker represent measurement accuracy in an order of hundredths of a millimeter and its price, which makes measurement expensive. Other measuring devices represent measurement arms [Nubiola 2013], ball bars, theodolites, indoor global positioning systems, coordinate measuring machines [Driels 1993], etc. The measurement of robot poses (position and orientation) can also be based on artifact measurement, where the robot can measure artifact geometry using a touch probe [Joubair 2015] or an artifact is attached to the robot flange and its position is measured using an external device. The design includes linear, planar, and 3-dimensional shapes. A precise artifact consisting of ellipsoidal, cylindrical, and spherical parts has been introduced [Kong 2022], where its position was measured using three laser displacement sensors. These methods require expensive equipment. [Legnani 2014] proposed a low-cost solution for pose measurements in the form of a wire sensor system. Not all robot configurations are suitable for measurement. An optimal configuration was presented by [Joubair 2015], and it describes an observability analysis based on a singular value decomposition of the Jacobian matrix.

Error identification is based on the optimization of an objective function that results from the model being used. The objective function is usually proposed as a sum of the distances between the model and the measured positions. This optimization problem can be combined with the neural network solution used to further improve accuracy [Monica 2003]. [Kong 2022] proposed a novel kinematic error compensation that implements machine learning for nonlinear-error compensation.

The last point of calibration represents the compensation and verification of the increased accuracy. Actually, there is no valid standard for measuring robot accuracy, because the standard [IOS 9283] was canceled in 2014 without any replacement. However, almost all papers focused on calibration contain the verification of industrial robots, where the accuracy before and after calibration is compared. The results differ a lot, but the mean error was reduced from 30% [Kong 2022] to 87% [Joubair, 2015]. An interesting comparison of the complete and kinematic

models was presented [Joubair 2013], where the mean position error decreased by 59% and 77%, respectively.

This paper presents a method for the calculation of nominal geometric parameter corrections, which aim to improve robot accuracy. The calculation is based on measuring the position of the end arm where only a single joint is moving and the demanded trajectory of the end arm is circular. At least three points are required for every single joint, and these points are used for circle identification, indicating the center point, radius and plane normal vector. Based on the identified circle values, the Denavit-Hartenberg parameters are evaluated, and the corrections are calculated as the difference between the calculated and nominal values. A slightly different approach is taken with flange geometry identification, which requires at least three identified circles. Chapter 2 describes the method of correction data calculation, Chapter 3 performs tests that include numerical simulations and industrial verification, Chapter 4 discusses the possibilities of the method, and Chapter 5 contains the conclusion.

2 GEOMETRIC CORRECTION IDENTIFICATION

The identification of a geometric correction is based on the evaluation of real geometry, where the correction is considered as the difference between the evaluated and the nominal robot geometry. This data is then uploaded in the form of a correction to the control system, assuming that the control system implements these corrections. Since all joints are rotational, moving only a single joint moves the flange along a circular trajectory. Consequently, the presented method requires a single joint movement starting from the first joint to the last one; for the flange geometry measurement, more points have to be provided. The artifact geometry must be known, and together with its position, represent the only data inputs for the method presented. The real geometry of the robot is calculated from the artifact position measurement, where the artifact is attached to the robot flange. The artifact is equipped with at least three reflectors, whose position is measured using a laser tracker.

2.1 Robot Kinematic Model Used

The kinematic model used in the robot´s control system calculates the transformation between joint rotation and the selected Cartesian coordinate system (CCS). There are more CCSs defined with respect to the selected application. The most used represent world, base, tool, and flange coordinate systems. However, the transformation principle is similar, and it is based on transformation matrices. The Denavit-Hartenbetg (DH) description utilized two translations and two rotations to transform between two consequent coordinate systems [Denavit 1955]:

$$T_{12} = T\varphi_z(\theta).Tz(d).Tx(a).T\varphi_x(\alpha), \qquad (1)$$

Where Tz, Tx is the transformation matrix for translation in the Z- and X-directions, respectively, and $T\varphi_z, T\varphi_x$ denotes the matrix for rotation about the Z- and X-axes. Parameters θ, d, a, α define the distance and angle for translation and rotation, respectively, see Fig. 1. Geometric error compensation is based on the correction of the nominal dimensions and joint axes relative positions by evaluated offsets. The resulting kinematic model for transformation between two consequent CCSs is derived in the form:

$$T_{12} = T\varphi_z(\theta + \theta_{off}).Tz(d + d_{off}).Tx(a + a_{off}).T\varphi_x(\alpha + \alpha_{off}), \qquad (2)$$

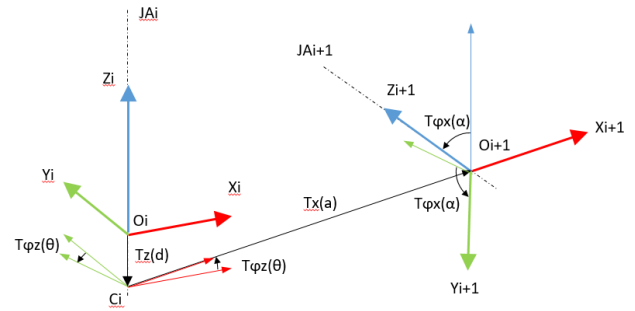where $\theta_{off}, d_{off}, a_{off}, \alpha_{off}$ represent offsets correcting the use of the nominal values.

Figure 1. Transformation from the ith joint to the following one based on the standard Denavit-Hartenberg kinematic description.

2.2 Circle Identification

Circle identification means the circle space position calculation in the form of the radius, center point, and plane of the circle. The circle is a planar entity which cannot be described by an equation in three dimensions. First, the measured points plane must be identified. This identification is based on the least-squares solution (LSS), where the plane minimizing normal distance from the points to the plane is calculated. Next, the measured points are transformed to the XY plane (see Fig. 2) using a transformation matrix T. This is calculated from the evaluated plane normal vector and the XY plane normal vector. After transformation of the measured points to the XY plane, the circle is identified as a result of residuum minimization:

$$Res = \sum_{i=1}^{N}\|(x_i - x_C)^2 + (y_i - y_C)^2 - r^2\|_2 \rightarrow min, \qquad (3)$$

where N denotes the number of measured points, (x_C, y_C), the circle center point, and r is the radius of the identified circle. The residuum solution uses the nonlinear least-squares solution. The coordinates of the identified center point are transformed to the measured plane using $S_0 = T^{-1}S_T$. Since the transformed matrix is orthonormal, the inverse of the matrix is equal to its transpositions $T^{-1} = T^T$.
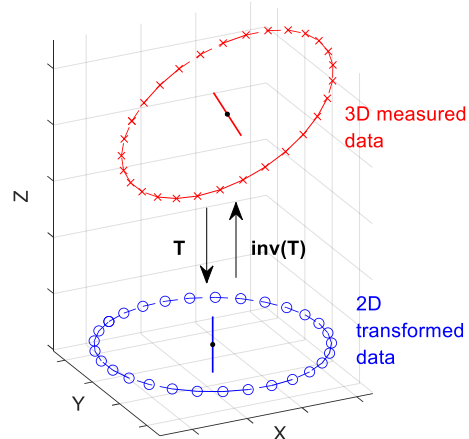

Figure 2. Fitting a circle to the measured points is based on transformation to the XY plane. The 3-dimensional points (red) and the transformed points (blue) are shown with the plane normal vectors. T denotes the kinematic transformed matrix.

2.3 Real Robot Kinematics Assembly

With all the circle parameters identified, the resulting kinematic model can be derived. First, all the normal vectors of the plane as well as the center points of the circle are transformed to set the center point of first joint to the global coordinate system origin, so its plane normal vector will be parallel to the Z-axis of the global coordinate system. The origin of the first coordinate

system is set to be the origin of the global coordinate system, and the joint rotation axis is identical to the Z-axis.

Based on the nominal kinematic model, every two consequent axes can be divided into perpendicular, parallel, and coincident groups, see Tab. 1. The kinematic transformation of both parallel and perpendicular axes is described in the following subsections.

Axis Pair	Kinematic configuration
1-2	Perpendicular
2-3	Parallel
3-4	Perpendicular
4-5	Perpendicular
5-6	Perpendicular
6-flange	Coincident

Table 1. Nominal axis kinematic configuration of every consequent axis pair of the considered industrial robot.

2.3.1 Transformation between perpendicular axes

Two axes perpendicular in the nominal robot kinematic model will probably not be perpendicular in the real robot. These skew axes will be nearly perpendicular, and it is here that the shortest distance defined by two points Ci and Ci+1 exists, see Fig. 1. The calculation of points Ci and Ci+1 represents a simple analytical task, and they are used for the calculation of DH parameters using the relations:

1. $\theta = \sphericalangle(C_{i+1} - C_i, x_i)$.
2. $d = k.\|C_i - O_i\|$, where constant k is given by the scalar product :
   $(Z_i).(C_i - O_i) > 0 \rightarrow k = 1$
   $(Z_i).(C_i - O_i) < 0 \rightarrow k = -1$
3. $a = \|O_{i+1} - O_i\|$.
4. $\alpha = \sphericalangle(JA_{i+1}, z_i)$.
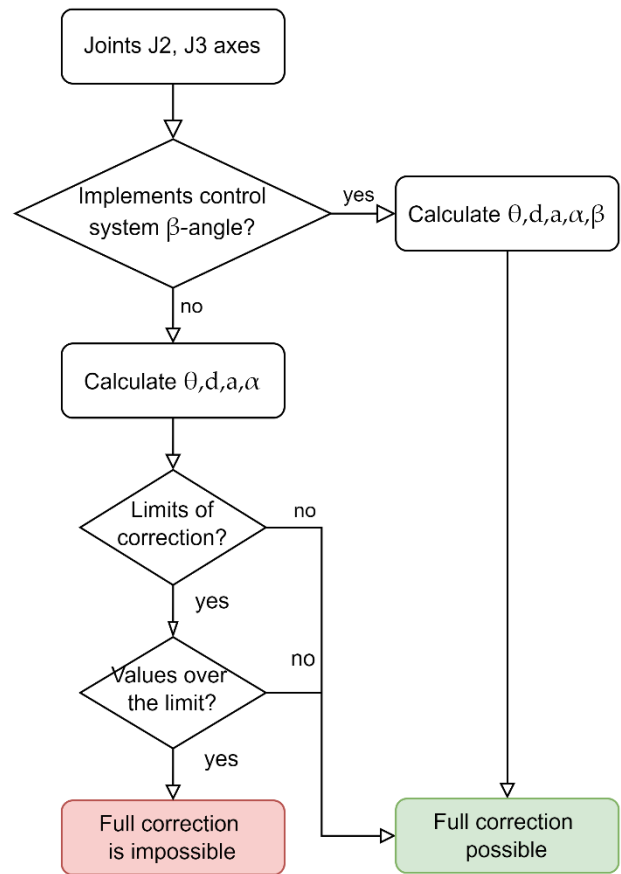
2.3.2 Transformation between parallel axes

If two consequent axes are parallel in the nominal kinematic model, the transformation between their CCSs will be calculated using a distinct algorithm, see flowchart in Fig. 3. If the identified axes are parallel, their distance will be given by points Ci, Ci+1. The point Ci is considered in the origin of the ith CCS, and the point Ci+1 defines the origin of the following CCS. The DH parameters are then calculated using the relations, and a full correction is possible.

1. $\theta = \sphericalangle(C_{i+1} - C_i, x_i)$.
2. $d = 0$.
3. $a = \|O_{i+1} - O_i\|$.
4. $\alpha = 0$.

If the axes are not parallel, they will either intersect each other or they will not. The transformation calculation depends on whether the robot control system implements a β angle. This angle extends standard DH parameters by Y-axis rotation, and it was introduced by [Hayati 1985] in the form of modified DH parameters. The kinematic transformation based on modified DH parameters can be expressed as:

$$T_{12} = T\varphi_z(\theta).Tz(d).Tx(a).T\varphi_x(\alpha).T\varphi_y(\beta). \qquad (4)$$

Using the β angle, a full correction is possible. If the control system does not implement the β angle, the transformation described in subsection 2.3.1 must be used. If the control system sets limit values for correction (e.g. Stäubli CS9 controller has a limit of ±200 mm for d translation corrections), then the full transformation will be impossible if the d translation is higher than the limit value.


Figure 3. Flowchart of the transformation for two nominal parallel axes. The algorithm selected depends on the control system and real relative axes geometry as well.

2.3.3 Transformation from J6 to flange

The last kinematic transformation relates to the 6th joint (J6) and flange geometry. But, the description is different from the previous two, since the flange and J6 are nominally coincident. However, the transformation must be identified, because J6 and the flange are not coincident in reality and all technologies and applications use the flange as a connecting interface. The flange itself is precisely manufactured, but the assembly may cause the Z6 and Z7 axes to not be coincident so that X6 and X7 are not parallel (Fig. 4). The principle of the transformation is based on the measurement of distinct points on the flange. At least the position of three points must be measured with an identical 6th joint rotation for flange plane evaluation, see Fig. 5.
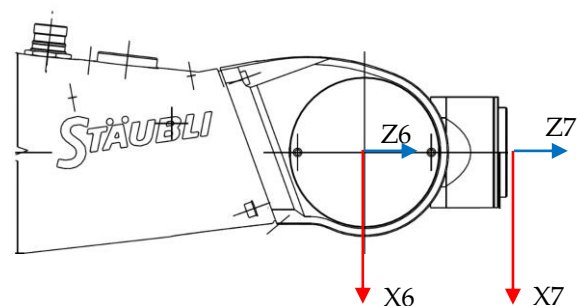
Figure 4. Coordinate systems of the 6th joint and the flange. Rotation of the flange is actuated by the 6th axis drive [Staubli 2022].
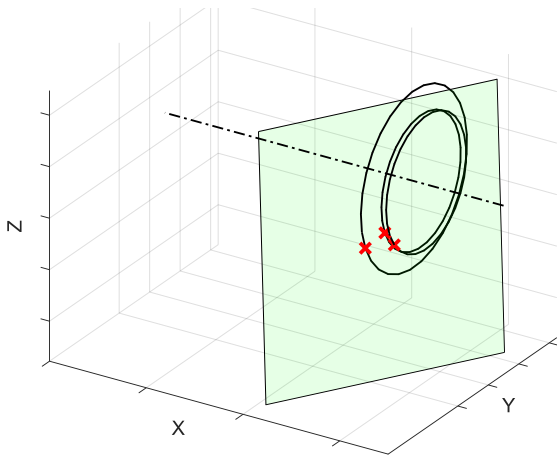
Figure 5. Transformation from 6th Cartesian coordinate system to the flange. At least three points on the flange must be measured (red crosses).

Rotation of the flange is actuated by the 6th joint, and the planes of the resulting circles will be perpendicular to this joint axis. The plane of the flange is calculated from at least the position of three points measured at the same 6th joint rotation as the cross product of the two vectors defined by the points measured $n = (P_2 - P_1) \times (P_3 - P_1)$. The coordinates of the measured points must be known in the flange coordinate system (x7,y7,z7). Based on the point's position with the known 6th axis rotation, the origin of 7th coordinate system is calculated as the intersection of spheres with their center points in the measured points and radii given by their position in the 7th CCS.

1. $\theta = \sphericalangle(O_7 - I_7, x_6)$, where I_7 denotes the intersection of the 6th joint axis and the perpendicular plane containing O_7.
2. $d = \|O_6 - I_7\|$.
3. $a = \|O_7 - I_7\|$.
4. $\alpha = \mathrm{arctg}(\frac{n_{rot\theta}(2)}{n_{rot\theta}(1)})$, where $n_{rot\theta} = T_{\varphi z}(-\theta).n$ is the plane normal vector rotated by $(-\theta)$ angle.
5. $\beta = \mathrm{arctg}\left(\frac{n_{rot\theta}(1)}{\|n_{rot\theta}(2),n_{rot\theta}(3)\|}\right)$.

### 2.4 Flange Position Measurement

Measurement of the flange position is essential for application of the proposed method. The position does not need to be measured in the robot coordinate system, since the circle planes are evaluated relative to the first one. Since the range of the robot motion is expected to be large and nonlinear, an efficient method for the position measurement would be a laser tracker or laser tracer. A laser tracker measures the 3-dimensional point position or only the point distance in case of a laser tracer, respectively. If a laser tracer device is used, the point's distance must be measured from distinct laser tracer positions, and the point position is evaluated using the multilateration principle. A laser tracker seems to be an efficient tool for position measurement, since only one laser tracker position is required. Thus, hereafter only a laser tracker will be considered; however, the principle is the same for a laser tracer. A laser tracker will measure the position of the spherical mounted reflector (SMR) attached to the flange. The position of the SMR on the flange must be known. It would be complicated to measure the position of the flange point directly, because some artifact holding the SMR attached to the flange is necessary and its geometry needs to be known.

The conventional methods for robot geometric error evaluation require either the point's position measurement in the robot coordinate system, or the transformation to the robot coordinate system as part of the solution. In both cases, it is not possible to distinguish between the flange and artifact real geometry, because these parameters are evaluated as a sum.

3 RESULTS

The proposed calibration method was tested in numerical simulations and subsequently with an industrial robot. In both cases, the Stäubli TX2-90 angular robot was selected as the use case. The numerical simulation contained both direct and inverse kinematic task solutions, where the direct method was used for simulation data calculations. The simulation data were calculated in two forms, where the first one involves nominal flange point measurement. Next, the flange point position was modified with respect to the typical accuracy of the flange point measurement to simulate real data acquisition. The industrial verification was based on an end effector position measurement using a laser tracker. The results are described in the following chapters.
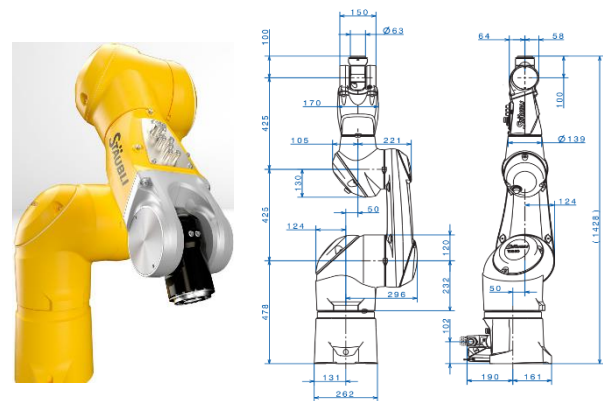
Figure 6. Stäubli TX2-90 industrial robot used within the numerical simulation and experimental verification [Staubli 2022]. The dimensions (right) were used to construct the nominal kinematic model.

3.1 Numerical Simulation with Nominal Points

Nominal measurement points can only be considered in a numerical simulation, and these points are defined without any measurement error. Their coordinates are only given by the robot and the artifact holding the reflector's geometry. Based on Fig. 6, the nominal DH parameters of the Stäubli TX2-90 were derived, and they are listed in Tab 2. The chosen offsets were added to these parameters to simulate real robot geometry. Using forward kinematics, artifact geometry (SMR1=[100 100 50] mm, SMR2=[80 125 50] mm, SMR3=[110 160 50] mm) and full joints rotation (J1=[-180 180] deg, J2=[-130 147.5] deg, J3=[-145 145] deg, J4=[-270 270] deg, J5=[-115 140] deg, J6=[-270 270] deg), the nominal point's position was calculated. The scope of the joint's rotation was divided into 30 positions, where the artifact positions were calculated. The identified circles are shown in the Fig. 7, and the difference between selected (Tab. 2) and identified robot geometry is given in Tab. 3.

Joint nr.	Theta [deg]	D [mm]	A [mm]	Alpha [deg]
1	0 - 0.22	0 - 0.16	50 + 0.11	-90 + 0.17
2	-90 - 0.21	0 - 0.15	450 + 0.12	0 + 0.18
3	90 - 0.20	50 - 0.14	0 + 0.13	90 + 0.19
4	0 - 0.19	425 - 0.13	0 + 0.14	-90 + 0.20
5	0 - 0.18	0 - 0.12	0 + 0.15	90 + 0.21
6	0 - 0.17	100 - 0.11	0 + 0.16	0 + 0.22

Table 2. Input kinematic parameters of the Stäubli TX2-90 robot used in the numerical simulation consist of nominal values (bold) and the offset.
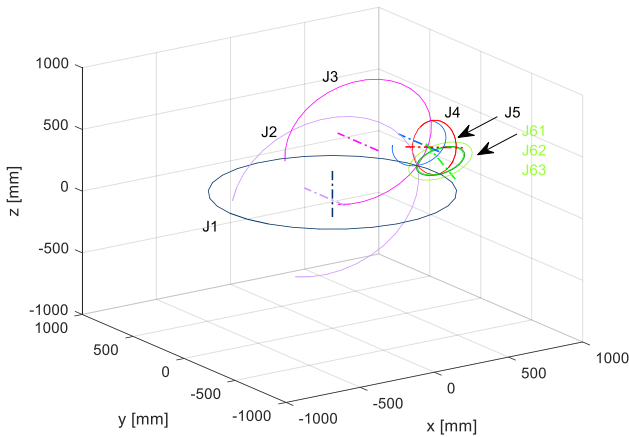
Figure 7. Numerical simulation of a single joint's rotation.

Joint nr.	Theta [deg]	D [mm]	A [mm]	Alpha [deg]
1	<1.10⁻⁹	<1.10⁻⁹	<1.10⁻⁹	<1.10⁻⁹
2	<1.10⁻⁹	<1.10⁻⁹	<1.10⁻⁹	<1.10⁻⁹
3	<1.10⁻⁹	<1.10⁻⁹	<1.10⁻⁹	<1.10⁻⁹
4	<1.10⁻⁹	<1.10⁻⁹	<1.10⁻⁹	<1.10⁻⁹
5	<1.10⁻⁹	<1.10⁻⁹	<1.10⁻⁹	<1.10⁻⁹
6	<1.10⁻⁹	<1.10⁻⁹	<1.10⁻⁹	<1.10⁻⁹

Table 3. Difference between the selected and identified robot geometry within the numerical simulation without any measurement error.

3.2 Numerical Simulation with Measurement Error

The point's prostitution without any measurement error may only be considered for numerical testing. Real measurement always considers finite accuracy depending on the method and devices used. The proposed method uses a laser tracker device (Leica AT 960), in which typical measurement uncertainty may be expressed as a function of SMR and laser tracker distance:

$$u = \pm(0.010 + 0.003d), \tag{5}$$

where the uncertainty u [mm] consists of a constant and a variable part. This depends on the distance of the laser tracker and the SMR distance d [m]. Based on equation (5) and the robot size, the distance was defined as d=5 m, resulting in ±0.025 mm uncertainty. The nominal measured points from Chapter 3.1 were combined with the normally distributed ±0.025 mm uncertainty, and the difference between selected (Tab. 2) and identified robot geometry is given in Tab. 4.

Joint nr.	Theta [deg]	D [mm]	A [mm]	Alpha [deg]
1	0.0000	0.0000	-0.0015	-0.0001
2	0.0008	0.0016	0.0074	0.0002
3	-0.00110	0.0020	0.0040	0.0006
4	0.0027	-0.0015	0.0050	-0.0024
5	-0.0020	0.0067	0.0064	0.0051
6	-0.0011	-0.0033	-0.0029	-0.0013

Table 4. Difference between the selected and identified robot geometry within the numerical simulation with measurement errors.

3.3 Industrial Verification

Industrial verification was performed using the Stäubli TX2-90, whose position was measured using a Leica AT960 interferometer. First, the artifact geometry was measured on the coordinate measuring machine (CMM) using a Renishaw

SP25M scanning probe (Fig. 8), where the center points of three spheres (i.e. the coordinates of the measured points) were evaluated with respect to the connection interface. Then, the artifact was mounted on the flange of the robot, and the laser tracker was placed in a suitable position for the measurement (Fig. 9). The initial robot position was set to J1=0°, J2=30°, J3=75°, J4=0°, J5=45° and J6=0°. From this position, the joints were consecutively rotated. The axes range was set with respect to artifact size, robot configuration, and experiment spatial distribution to J1=(-30°,+180°), J2=(-105°,+65°), J3=(-120°,+130°), J4=(-10°,+200°), J5=(-100°,+100°) and J6=(-90°,+270°). These ranges were divided into 20 intervals, resulting in 21 measured points for every joint. The robot program was developed in the Stäubli Robotic Suite environment, where a delay of 10 seconds was set after reaching the target position. Such a delay is high enough for precise measurement and has to been implemented as a constant value, since no communication between the robot controller and the laser tracker was established. The 0.5" SMRs have an acceptance angle of ±30°, and they need to be rotated so as not to interrupt the laser beam during the measurement. The reflectors are held in precise magnetic seats, which enables the rotation of the reflectors without a loss of precision. However, not all kinematic configurations reflected the beam back to the laser tracker, and these positions (5 of 168) have not been measured.
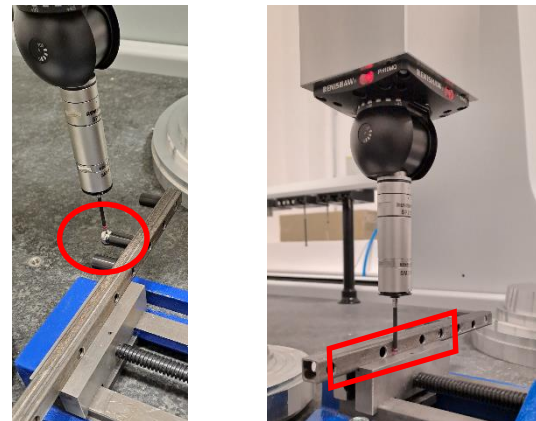

Figure 8. The artifact holds the reflectors and its geometry was measured on a coordinate-measuring machine. The geometry measurement consists of sphere center (left) and basic plane evaluation (right).
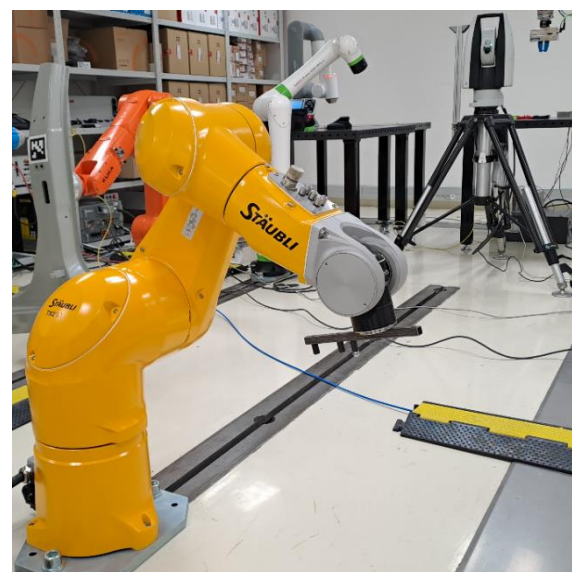

Figure 9. Industrial verification with the Stäubli TX2-90 robot. The artifact attached to the robot flange was measured by the laser tracker Leica AT 960.

Based on the measured data, the DH parameters were calculated, and these were compared to their nominal values. Their offsets were evaluated, and updates were made in the control system. There are two approaches for the updates in the DH offsets in the robot Staubli controller:

1. Generate a program with the *setDH (theta, d, a, b, alpha, beta)* function, in which parameters represented the updated DH offsets.
2. Modify the configuration file arm.cfx, where the offsets are listed in array form (in the following sample, all offsets are zero, and parameter *b* is not implemented in the control system):

```
<DhArray name="dhOffset" >
<DH index="0" theta="0" d="0" a="0" b="0" alpha="0" beta="0" />
<DH index="1" theta="0" d="0" a="0" b="0" alpha="0" beta="0" />
<DH index="2" theta="0" d="0" a="0" b="0" alpha="0" beta="0" />
<DH index="3" theta="0" d="0" a="0" b="0" alpha="0" beta="0" />
<DH index="4" theta="0" d="0" a="0" b="0" alpha="0" beta="0" />
<DH index="5" theta="0" d="0" a="0" b="0" alpha="0" beta="0" />
</DhArray>
```

Compared to the numerical simulation, the impact of identified DH offsets can only be evaluated for robot positioning accuracy, because the real parameters are not known. The end effector position is measured with the laser tracker as well, but the laser tracker and robot coordinate systems must be aligned to compare the nominal and real positions. Coordinate system alignment is based on the measurement of the N-points position with the laser tracker and the calculation of the transformation matrix between the robot and the laser tracker coordinate system. At least four points are required for the calculation. Although more approaches exist for the transformation matrix calculation, the quaternion-based solution was utilized [Horn 1987]. Using the calculated transformation matrix, the values from the laser tracker are transformed to the robot coordinate system, and these values may be directly compared to the nominal robot position. Alignment is calculated from the measurement of eight points, where all joints move simultaneously. Verification of the proposed method was based on the measurement of ten points, both with and without the corrections. The results are shown in the Fig. 10.
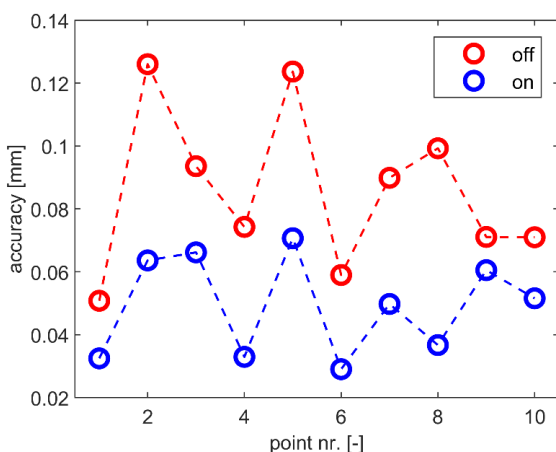
4 DISCUSSION

The numerical simulation verified the proposed method with very promising results. In the simulation, the DH parameters are known, and the flange position was calculated using forward kinematic solutions. If the nominal flange position is considered, the DH parameters will be identified with an accuracy of the numeric rounding error ($<<1.10^{-9}$ mm). Considering typical laser tracker measuring accuracy, the DH parameters were identified with very high precision as well, where the difference between the selected and identified parameters was still negligible. Industrial verification requires a different approach in evaluation, since the real DH parameters are not known. The approach is based on the measurement of the flange position and the calculated deviation of the set versus the actual value. Without the corrections, the mean and maximal deviations were 0.086 mm and 0.126 mm, respectively. After activating the corrections, these deviations decreased to 0.049 mm and 0.070 mm, respectively. Concluding the verification, the absolute position accuracy was increased by 43%. This improvement is significant. However, it is worth mentioning that the Stäubli TX2-90 robot is already highly precise, even without the corrections. The manufacturer ensures a repeatability of 0.030 mm [Staubli 2022].

The main advantage of the proposed method represents its simplicity, since only the basic least-squares solution and linear algebra are required for its implementation. The next advantage comes from the principle method, where the measured points are not directly used for the correction calculation. Instead, they are used to construct derived geometric entities (circles). Also, because only tens of points are used for every single circle calculation, the result is identified with high accuracy. Another advantage is that the laser tracker measurement is made without the need for coordinate system alignment, because the relative position of the circles to the first one is evaluated. Finally, an advantage worth noting is the identification of the complete flange geometry, where some traditional methods cannot identify the full flange geometry, e.g. the axial offset of 6th joint is evaluated as a sum of robot and artifact geometry.

The main drawback is the need for artifact metrology measurement, because its geometry has to be identified. The artifact should be made of thermally invariant material, or it should be inspected within the same environmental conditions to achieve the highest accuracy. However, the artifact geometry only needs to be known for flange full geometry identification. The other joints are identified without the need for artifact geometry knowledge. The laser tracker required for the measurement is an expensive device, but so are the state-of-art calibration methods usually used in lieu of it.

Follow-up research will be focused on the implementation of the proposed method onto the control systems, which do not allow the corrections of the kinematic model to be calculated. The implementation may be processed using two distinct methods. The first method is based on an offline robot trajectory modification using the corrected kinematic model. The second method calculates the modified positions online in a separate industrial computer, where it is connected to the robot control system and the robot is operated in an external automatic mode.

5 CONCLUSIONS

This article describes a method for increasing industrial robot positioning accuracy. The method is based on the correction of nominal kinematic model parameters like traditional calibration methods; however, the novelty comes from the method of the offsets calculation. The method was successfully verified by a numerical simulation and industrial verification with a Stäubli TX2-90 as well. The summary points of the proposed calibration can be defined as:

- The proposed method does not improve repeatability, it only increases industrial robot positioning accuracy;
- The robot control system must implement corrections to the nominal kinematic model;
- The geometry of the artifact mounted to the end effector must be known;
- The position of the artifact mounted to the robot end effector must be measured (e.g. with a laser tracker);
- Artifact position may be related to an arbitrary coordinate system, no laser tracker-robot alignment is needed;
- The measured points themselves are not used in the calibration - they are simply used to build dervied geometric entities (circles) which are then used to increase the accuracy of the proposed method.

The algorithmization of the proposed method is not difficult, and it allows full user control over the calculation. Based on this method, the calibrated robots achieve the higher positioning accuracy required for high accuracy application utilization.

ACKNOWLEDGMENTS

REFERENCES

[Denavit 1955] Denavit, J. and Hartenberg, R.S. A Kinematic Notation for Lower-Pair Mechanism Based on Matrices. Journal of Applied Mechanics 1955, 22, 215–221, doi:10.1115/1.4011045.

[Driels 1993] Driels, M.R. et al. Full-Pose Calibration of a Robot Manipulator Using a Coordinate-Measuring Machine. Int J Adv Manuf Technol 1993, 8, 34–41, doi:10.1007/BF01756635.

[Hayati 1985] Hayati, S. and Mirmirani, M. Improving the Absolute Positioning Accuracy of Robot Manipulators. J. Robotic Syst. 1985, 2, 397–413, doi:10.1002/rob.4620020406.

[Horn 1987] Horn, B.K.P. Closed-Form Solution of Absolute Orientation Using Unit Quaternions. J. Opt. Soc. Am. A 1987, 4, 629, doi:10.1364/JOSAA.4.000629.

[ISO 9283] ISO 9283:1998(E) Manipulating industrial robots – Performance criteria and related test methods, 1998-04-01.

[Joubair 2013] Joubair, A. et al. Calibration Efficiency Analysis Based on Five Observability Indices and Two Calibration Models for a Six-Axis Industrial Robot. SAE Int. J. Aerosp. 2013, 6, 161–168, doi:10.4271/2013-01-2117.

[Joubair 2015] Joubair, A. and Bonev, I. A. Kinematic calibration of a six-axis serial robot using distance and sphere constraints. Int J Adv Manuf Technol 2015, 77, 515-523, doi: 10.1007/s00170-014-6448-5.

[Kong 2022] Kong, L.-B. and Yu, Y. Precision Measurement and Compensation of Kinematic Errors for Industrial Robots Using Artifact and Machine Learning. Adv. Manuf. 2022, 10, 397–410, doi:10.1007/s40436-022-00400-6.

[Legnani 2014] Legnani, G. and Tiboni, M. Optimal Design and Application of a Low-Cost Wire-Sensor System for the Kinematic Calibration of Industrial Manipulators. Mechanism and Machine Theory 2014, 73, 25–48, doi:10.1016/j.mechmachtheory.2013.09.005.

[Monica 2003] Monica, T et al. A Closed-Loop Neuro-Parametric Methodology for the Calibration of a 5 DOF Measuring Robot. In Proceedings of the Proceedings 2003 IEEE International Symposium on Computational Intelligence in Robotics and Automation. Computational Intelligence in Robotics and Automation for the New Millennium (Cat. No.03EX694); IEEE: Kobe, Japan, 2003; Vol. 3, pp. 1482–1487.

[Nubiola 2013] Nubiola, A. and Bonev, I.A. Absolute Calibration of an ABB IRB 1600 Robot Using a Laser Tracker. Robotics and Computer-Integrated Manufacturing 2013, 29, 236–245, doi:10.1016/j.rcim.2012.06.004.

[Roth 1987] Roth, Z.; Mooring, B.; Ravani, B. An Overview of Robot Calibration. IEEE J. Robot. Automat. 1987, 3, 377–385, doi:10.1109/JRA.1987.1087124.

[Staubli 2022] Staubli. TX2-90 industrial robot range. Staubli, 2022 [online]. Oct. 5, 2022 [date of citing Oct 27, 2022]. Available from <https://www.staubli.com/hu/en/robotics/products/industrial-robots/tx2-90.html >.

[Zippia 2022] McCain A. 25 Revolutionary robotics industry statistics [2022]: Market size, growth, and biggest companies. Zippia, 2022 [online]. Oct. 5, 2022 [date of citing Oct 27, 2022]. Available from <https://www.zippia.com/advice/robotics-industry-statistics/>.

CONTACTS:

Czech Technical University in Prague, Faculty of Mechanical Engineering, Department of production machines and equipment (RCMT), Horská 3, 128 00 Praha, Czech Republic; Website : https://rcmt.cvut.cz/

Ing. Stepan Chladek, Ph.D.   **Ing. Jiri Sveda, Ph.D.**
E: s.chladek@rcmt.cvut.cz   E: j.sveda@rcmt.cvut.cz

Czech Technical University in Prague, Faculty of Mechanical Engineering, Department of Mechanics, Biomechanics and Mechatronics, Technicka 4, 166 07 Praha 4, Czech Republic; Website : https://mech.fsid.cvut.cz/

Prof. Ing. Zbynek Sika, Ph.D.   **Ing. Petr Benes, Ph.D.**
E: zbynek.sika@fs.cvut.cz   E: petr.benes@fs.cvut.cz